



Synthesis of mono and doubly alkynyl substituted ferrocene and its crystal engineering using $-C-H\cdots O$ supramolecular synthon

Arunabha Thakur^a, N.N. Adarsh^{b,1}, Amarnath Chakraborty^{b,1}, Manjula Devi^a, Sundargopal Ghosh^{a,*}

^a Department of Chemistry, Indian Institute of Technology Madras, Chennai 600036, India

^b Department of Organic Chemistry, Indian Association for the Cultivation of Science, Kolkata 700032, India

ARTICLE INFO

Article history:

Received 10 October 2009

Received in revised form 14 November 2009

Accepted 15 November 2009

Available online 20 November 2009

Keywords:

Ferrocene

Alkynyl ferrocene

C–H \cdots O interaction

ABSTRACT

Mono and doubly alkynyl substituted ferrocene complexes, $[Fc(CH_2OCH_2C\equiv CH)_n]$, **2–3** (**2**: $n = 1$; **3**: $n = 2$; Fc = ferrocene) have been synthesized from the room temperature reaction of mono and 1,1'-dihydroxymethyl ferrocene, $Fc(CH_2OH)_n$, **1a–b** (**1a**: $n = 1$; **1b**: $n = 2$) and propargyl bromide, in modest to good yields. These new ferrocene derivatives have been characterized by mass, IR, 1H , ^{13}C NMR spectroscopy, and molecular structures of compound **2** and **3** were unequivocally established by single crystal X-ray diffraction study. The crystal structure analysis revealed that **2** and **3** consist of infinite 1D zig-zag hydrogen bonded chains and 2D microporous hydrogen bonded network of molecules, linked by intermolecular C–H \cdots O hydrogen bonding. The molecular structures of both **2** and **3** are further stabilized by C–H $\cdots\pi$ interactions.

© 2009 Elsevier B.V. All rights reserved.

1. Introduction

Among the various types of intermolecular interactions, the hydrogen bond is undoubtedly, the most important in terms of its contributions towards the stability and integrity of molecular and supramolecular structures [1–3]. In recent times, there has been a great deal of interest in weak hydrogen bonds formed by hydrogen atoms covalently bonded to carbon atoms [3]. The hydrogen atom in a terminal alkyne group is relatively acidic due to the sp hybridization and forms stronger C–H \cdots X hydrogen bonds than most hydrocarbon donors, with either an electronegative atom (e.g., O or N) or the π electron concentration of another $C\equiv C$ bond acting as the acceptor [4]. The crystal structure of terminal alkynes is becoming the focus of an increasing number of studies, with particular reference to their applicability in crystal engineering [5–8]. Modern crystal engineering has emerged as a wealthy discipline whose success requires an iterative process of synthesis, crystallography and crystal structure analysis. The $C\equiv C-H\cdots O_2N$ and $C\equiv C-H\cdots NC$ hydrogen bond motifs have been defined as supramolecular synthons by Desiraju and co-workers [9].

On the other hand, the chemistry of transition metal complexes, particularly those containing redox-active fragments such as the ferrocenyl group, remains an important research area [10–14] and is increasingly being investigated for a variety of potential

uses, such as those in the field of catalysis and development of novel materials [15–17] including materials for non-linear optics [18–20]. The reactivity of ferrocenyl alkynes has recently been investigated by Fehlner in detail with $[1,2-(\eta^5-C_5Me_5RuH)_2B_3H_7]$ to generate ruthenacarboranes [21] (Scheme 1). We, on the other hand, envisaged use of mono and doubly alkynyl substituted ferrocene, **2–3** to generate ruthenacarborane derivatives. While we successfully synthesized the compounds, **2** and **3**, interesting structural features were observed in their crystal structure. In this paper, we provide an account of the synthesis and characterization of compounds **2** and **3**, along with their crystal structure details and supramolecular architecture resulting from non-covalent, intermolecular, weak bonding interactions.

2. Result and discussion

2.1. Synthesis and characterization of $Fc(CH_2OCH_2C\equiv CH)$, **2**

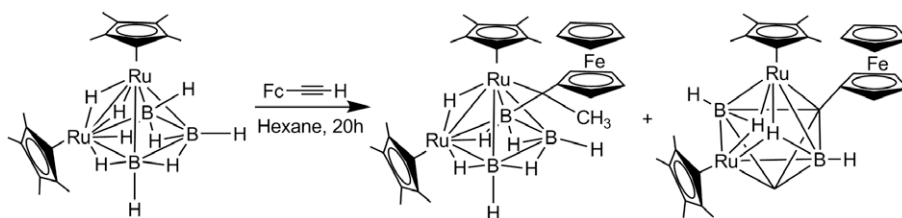
As shown in Scheme 2, the mono-alkyne derivative of ferrocene, **2** was synthesized by the reaction of propargyl bromide and **1a** in DMSO in presence of 1.2 equivalent of NaOH at room temperature.

Composition of **2** was defined by mass spectrometry, the molecular ion peak depicting an isotopic distribution pattern characteristic of one Fe and one oxygen atom. The IR spectrum of **2** is distinguished by the presence of an absorption band at 2171 cm^{-1} due to the presence of $C\equiv C$ bond. The acetylenic hydrogen has also been confirmed by 1H NMR, which shows the characteristic peak at δ 2.37 ppm. 1H NMR spectrum also shows the presence of two cyclopentadienyl rings (9H) of ferrocene in

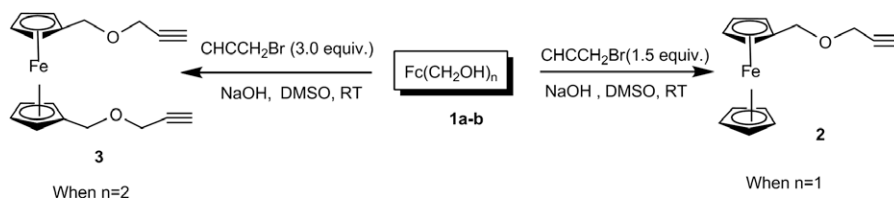
* Corresponding author. Tel.: +91 44 2257 4230; fax: +91 44 2257 4202.

E-mail address: sghosh@iitm.ac.in (S. Ghosh).

¹ Fax: +91 33 2473 2805.



Scheme 1. Synthesis of *nido*-1,2-(Cp^{*}Ru)₂(1,5-μ-C(Fc)Me)B₃H₇ and *closo*-4-Fc-1,2-(Cp^{*}Ru)₂-4,6-C₂B₂H₃ from ruthenaborane.



Scheme 2. Synthesis of mono- and doubly-alkyne substituted ferrocene, **2** and **3**.

the region δ 4.08–4.17 ppm and two protons (OCH₂ group) at δ 4.04–4.31 ppm region. The presence of all the characteristic peaks was further supported by ¹³C NMR spectrum. The crystal structure of **2**, shown in Fig. 1, confirms the structural assignment made on the basis of spectroscopic results. The C≡C bond distance of 1.186(4) Å in **2** (C13–C14, in Fig. 1) is consistent with the linear arrangement of acetylene.

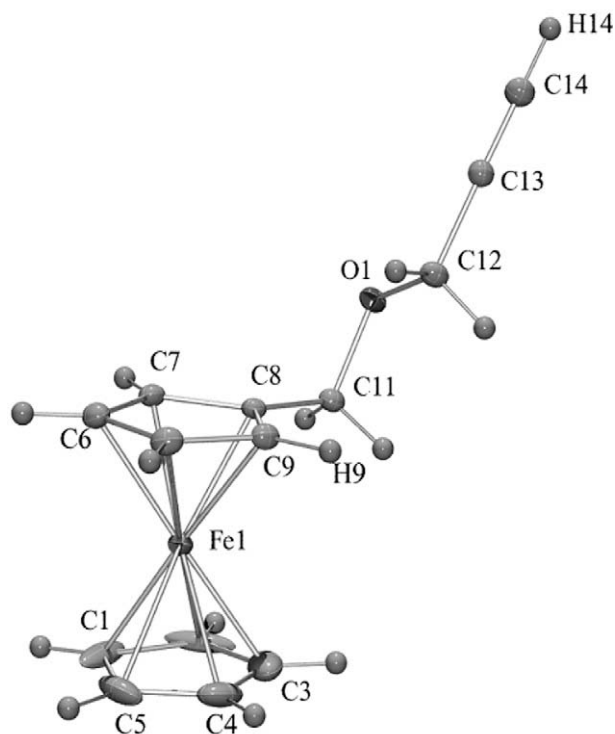


Fig. 1. Molecular structure of Fe(η^5 -C₅H₅)(η^5 -C₅H₄)(CH₂OCH₂CCH), **2** with thermal ellipsoid drawn at the 30% probability level. Selected bond length (Å) and angles (°): C(3)–Fe(1) 2.019(4), C(1)–Fe(1) 2.020(3), C(2)–Fe(1) 2.019(3), C(7)–Fe(1) 2.045(3), C(8)–Fe(1) 2.034(3), C(9)–Fe(1) 2.036(3), C(6)–Fe(1) 2.057(3), O(1)–C(12) 1.425(4), C(1)–C(5) 1.425(7), C(9)–H(9) 0.9800, C(14)–H(14) 0.9300; C(3)–Fe(1)–C(2) 39.4(2), C(2)–C(3)–Fe(1) 70.3(2), C(3)–Fe(1)–C(8) 109.85(14), C(1)–Fe(1)–C(9) 176.04(15), C(12)–C(13)–C(14) 178.4(3).

2.2. Synthesis and spectroscopic characterization of Fc(CH₂OCH₂-C≡CH)₂, **3**

Room temperature reaction of **1b** with a three fold excess of propargyl bromide in presence of NaOH yielded yellow alkynyl substituted ferrocene, Fc(CH₂OCH₂C≡CH)₂, **3** in good yield (Scheme 2). Compound **3** has been characterized by mass spectrometry, IR and multinuclear NMR spectroscopy and single crystal X-ray diffraction studies. Description of the characterization of **3** as follows.

The composition of **3** was confirmed by FAB mass spectrometry which shows the molecular ion peak at m/z 323. As observed in **2**, the IR spectrum of **3** features an absorption band at 2121 cm⁻¹ due to C≡C bond. The symmetrical ¹H NMR spectral pattern shows the presence of cyclopentadienyl rings protons (8H), two equivalents of characteristic acetylenic protons peak at δ 2.46 ppm, and two sets of OCH₂ groups in the region of δ 4.13–4.37 ppm. Corresponding peaks were observed in the ¹³C NMR spectrum. The spectroscopic data are consistent with the solid state X-ray structure which is shown in Fig. 2. The C≡C bond distance of 1.181(19) Å and the bond angle of 177.9(15)° in **3** are comparable with that of **2**. The acetylenic bond angle is comparable to other ferrocenyl alkyne molecules [22–29], e.g., C(Fc)₂(OCH₃)(C≡CH) (177.6) [28], C(Fc)(OCH₃)(Ph)C≡C(Ph)(OH)Fc (177.3°) [29].

In ferrocene, the UV–Vis spectrum shows two absorption bands. The band at 442 nm is due to the lower energy transition (¹E_{1g} ← ¹A_{1g}) and 325 nm is due to the higher energy transition (¹E_{2g} ← ¹A_{1g}). The UV–Vis spectrum changes dramatically upon substitution of the cyclopentadienyl ring with conjugated and/or acceptor groups, as was observed when an alkoxy Fischer carbene complex, [(CO)₅M=C(OCH₃)(-CH=CH-)_n(C₅H₄)Fe(C₅H₅), M = W, Cr, $n = 1$ –4] was attached to the Cp ring of ferrocene [30]. However, the effect is not significant while the ferrocene ring is substituted by unconjugated acceptor or donor groups. This is evident from the UV–Vis spectrum of **2** and **3**, shown in Fig. 3.

2.3. Description of the crystal structures of alkynyl substituted ferrocene complexes **2**, **3**

The alkyne substituted functionality in **2** and **3** [–C≡C–H...O–(R)₂ (where O–(R)₂ is ether functional group)] is responsible for the C–H...O interactions that lead to the formation of hydrogen

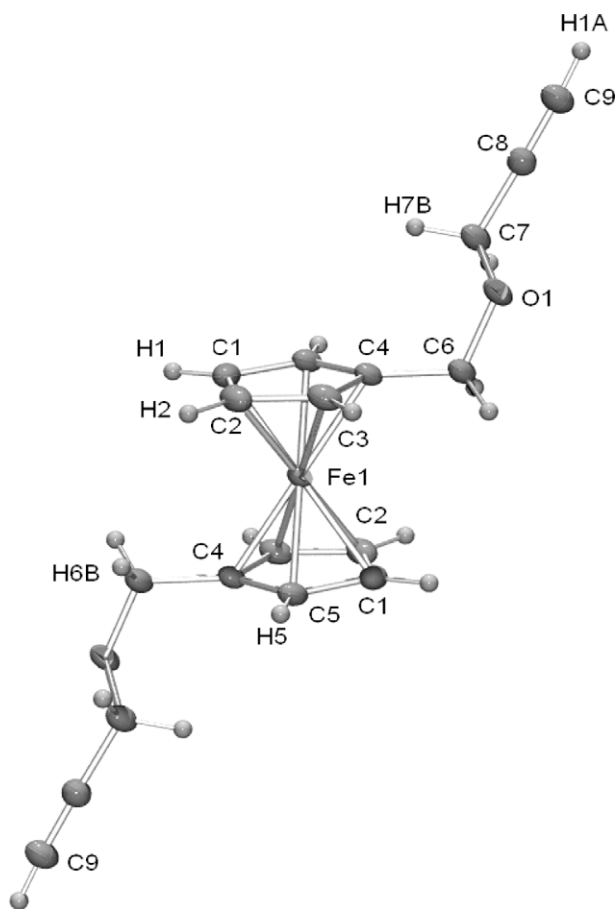


Fig. 2. Molecular structure of $\text{Fe}(\eta^5\text{-C}_5\text{H}_4)_2(\text{CH}_2\text{OCH}_2\text{CCH})_2$, **3** with thermal ellipsoid drawn at the 30% probability level. Selected bond length (Å) and angles ($^\circ$): C(3)–Fe(1) 2.0456(13), C(1)–Fe(1) 2.0393(12), C(4)–Fe(1) 2.0456(13), C(5)–Fe(1) 2.0366(11), C(7)–O(1) 1.4224(15), O(1)–C(6) 1.4412(15), C(5)–C(6) 1.4943(17), C(7)–H(7A) 0.99, C(4)–H(4) 0.99, C(9)–H(1X) 0.87(3); C(3)–C(2)–Fe(1) 69.72(7), C(6)–C(5)–Fe(1) 123.06(8), O(1)–C(6)–C(5) 113.55(10), C(7)–C(8)–C(9) 177.90(15).

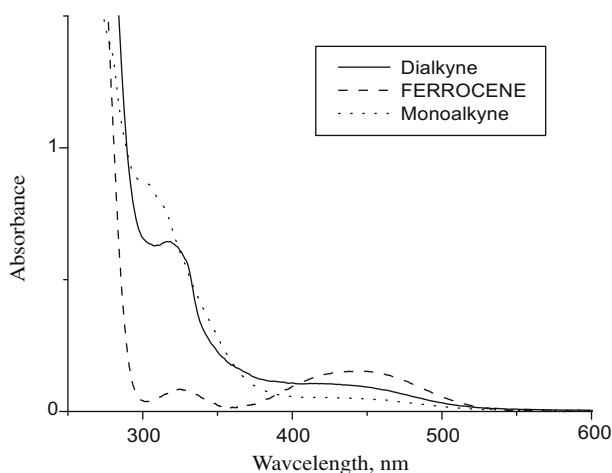


Fig. 3. UV-Vis spectra of ferrocene, **2** and **3** in CH_3CN solution.

bonded networks 1D zig-zag and 2D microporous sheet in **2** and **3** respectively. The compound **2** got crystallized in centrosymmetric monoclinic space group $P2_1/c$ whereas the compound **3** in monoclinic space group $P2_1/n$. In the asymmetric unit of **2**, one full molecule was found and one half of the molecule was found

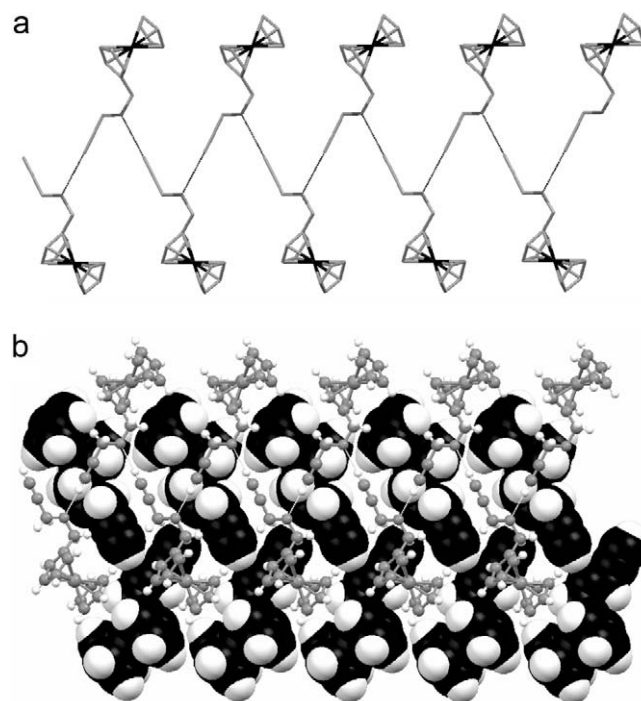


Fig. 4. Crystal structure illustration of **2**: (a) 1D zig-zag hydrogen bonded network via C–H...O. (b) Offset packing of **2** in the crystal lattice stabilized by C–H...O and C–H... π interactions.

(located on the inversion center) for the compound **3**. The acidic hydrogen in a terminal alkyne group forms stronger C–H...X hydrogen bonds than most hydrocarbon donors, with either an electronegative atom (e.g., O or N) or the π electron cloud of the $\text{C}\equiv\text{C}$ bond acting as the acceptor.

In the crystal structure of **2**, C–H of the alkyne functionality is involved in hydrogen bonding with O of the ether functionality via C–H...O interaction [$\text{C}\cdots\text{O} = 3.166(4) \text{ \AA}$; $\angle\text{C–H}\cdots\text{O} = 166(2)^\circ$] resulting in the formation of a 1D zig-zag hydrogen bonded network with micropores (Fig. 4). Each such 1D network is further stabilized by C–H... π interaction [31,32] [$\text{C}\cdots\pi = 3.644\text{--}3.786$] (Fig. 5) and due to the offset packing, the micropores are filled by adjacent 1D zig-zag layers (Fig. 4).

In the crystal structure of **3**, the C–H of the alkyne functionality is also involved in hydrogen bonding with the O of ether functionality via C–H...O interaction [$\text{C}\cdots\text{O} = 3.181(16) \text{ \AA}$; $\angle\text{C–H}\cdots\text{O} = 166(3)^\circ$] resulting in the formation of a 2D hydrogen bonded microporous network (view down crystallographic axis c) (Fig. 6). The micropores, however, are filled by adjacent layers because of offset packing via C–H... π interactions [31,32] involving C–H of $-\text{CH}_2-$ with π electron cloud of cyclopentadienyl ring and alkyne. [$\text{C}\cdots\pi = 3.703\text{--}3.787 \text{ \AA}$] (Figs. 6 and 7).

2.4. Electrochemical study

The electrochemical property of the redox-active ferrocene moiety and its derivatives, **2** and **3** has been studied by cyclic voltammetry (CV). Cyclic voltammograms of ferrocene, **2** and **3** in $\text{Bu}_4\text{NClO}_4\text{-MeCN}$ are shown in Fig. 8, showing one electron oxidation and reversible one electron reduction waves in the potential range between 0 and 1.0 V vs. SCE for both complexes. The CV showed a reversible redox couple of ferrocene/ferrocenium at $E_{\text{Fc}/\text{Fc}^+}^0 = (E_{\text{pa}} + E_{\text{pc}})/2 = 0.395 \text{ V}$ for ferrocene, 0.493 V for **2** and 0.532 V for **3**. An increase in potential value is generally associated with an electron-acceptor property of the substituent [33,34]. Therefore the gradual increase of the E^0 value of compound **2**

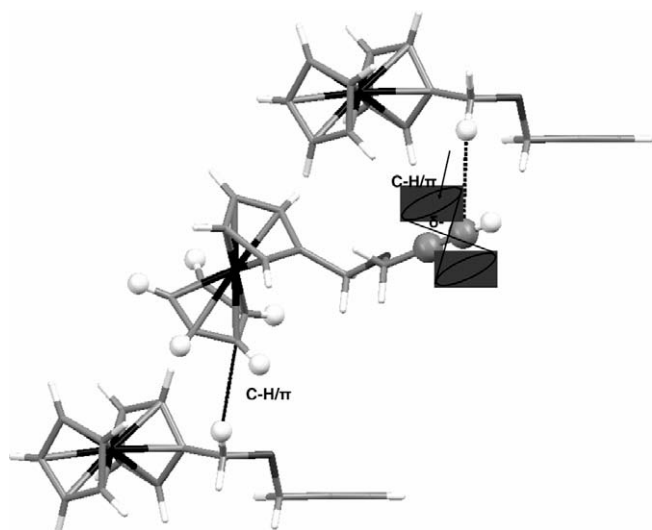


Fig. 5. Crystal structure illustration of **2**: C–H... π interaction in the crystal structure.

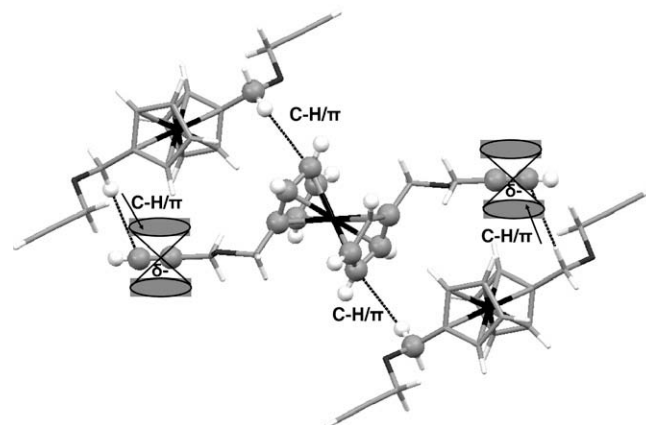


Fig. 7. Crystal structure illustration of **2**: C–H... π interaction in the crystal structure.

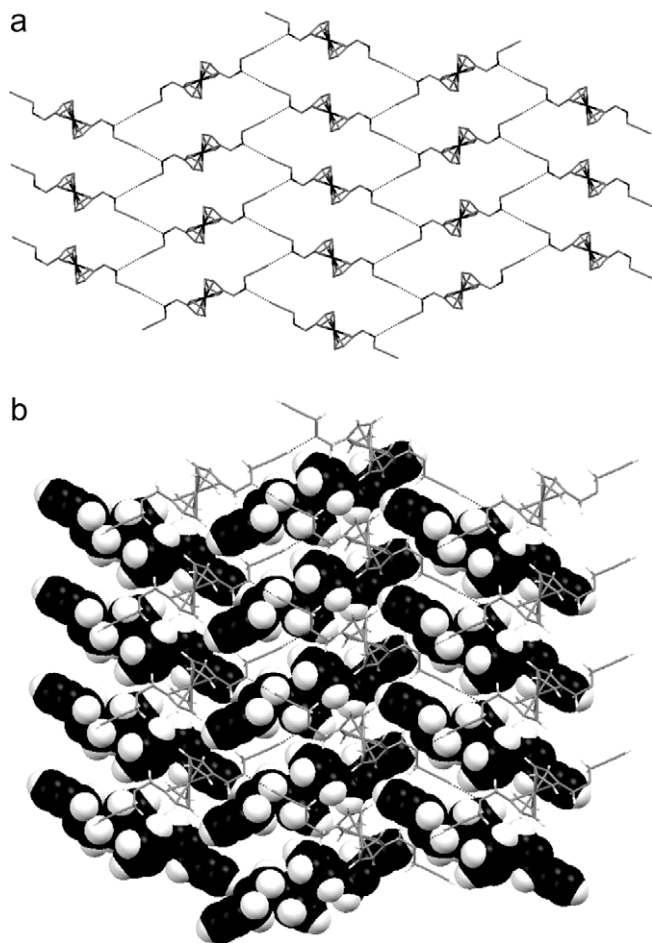


Fig. 6. Crystal structure illustration of **2** (a) 2D hydrogen bonded network of **2** via C–H...O interaction; (b) offset packing of two adjacent 2D hydrogen bonded networks.

and **3** from the ferrocene moiety clearly indicates the electron-acceptor property of the alkyne ether linkage attached to the ferrocene unit.

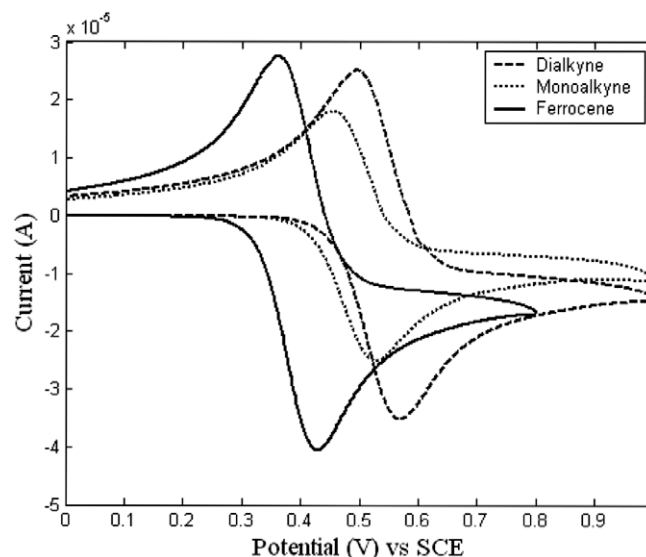


Fig. 8. Cyclic voltammograms of ferrocene, **2** and **3** at glassy carbon in 0.1 M Bu₄NClO₄ as supporting electrolyte and acetonitrile as solvent. The scan rate employed as 0.1 V s⁻¹.

3. Conclusions

In conclusion, we have demonstrated a facile, efficient synthesis of mono- and doubly-alkynyl substituted ferrocene complexes **2** and **3**. The alkyne functionality in **2** and **3** are responsible for the C–H...O interactions (–C≡C–H...O supramolecular synthon) which leads to the formation of 1D zig-zag hydrogen bonded microporous network in **2** an 2D hydrogen bonded microporous network in **3**. The synthetic utility of the products has been demonstrated and their electrochemical property was evaluated by CV studies. Further work on these compounds for the preparation of metallacarboranes of early transition metals (e.g., V, Nb or Ta), and possible utilization as ligands in catalytic organic reactions are in progress.

4. Experimental

4.1. General procedures and instrumentation

All the operations were conducted under an Ar/N₂ atmosphere using standard Schlenk techniques and Glove Box. Solvents were distilled and degassed prior to use under Argon. propargyl

bromide, butyl lithium, tetramethylethylenediamine (TMEDA) (Aldrich), tetrabutyl ammonium bromide, allyl bromide, ferrocene purchased were of analytical grade and used without further purification. DMF purchased from Aldrich and freshly distilled prior to use. Mono and 1, 1'-dihydroxymethyl ferrocene complexes, **1a–b** were prepared according to the literature [35,36]. Chromatography was carried out on 3 cm of silica gel in a 2.5 cm diameter column. Thin layer chromatography was carried on 250 mm diameter aluminum supported silica gel TLC plates (MERK TLC Plates). NMR spectra were recorded on 400 or 500 MHz Bruker FT-NMR spectrometer. Infrared spectra were obtained on a Nicolet 6700 FT-IR spectrometer. Crystal data were collected and integrated using Bruker Apex II CCD area detector system equipped with graphite monochromated Mo K α ($\lambda = 0.71073 \text{ \AA}$) radiation at 150 K.

4.2. Synthesis of Fc(CH₂OCH₂C \equiv CH), **2**

A solution of **1a** (0.5 g, 2.3 mmol) in 15 ml DMSO was treated with NaOH (0.11 g, 2.76 mmol) at room temperature for 30 min. Propargyl bromide (0.4 ml, 3.45 mmol) was added dropwise to the reaction mixture and stirred for 24 h. The reaction mixture was diluted with 10–15 ml of cold water and extracted with EtOAc. The organic layer was dried over anhydrous Na₂SO₄ and solvent was removed under reduced pressure. The pure product was isolated by silica gel column chromatography and elution with EtOAc:hexane (25:75 v/v) yielded yellow Fc(CH₂OCH₂C \equiv CH), **2** (0.29 g, 50%).

4.2.1. Compound **2**

MS (FAB) P⁺(max): *m/z* (%) 255; ¹H NMR (400 MHz, CDCl₃, 22 °C): $\delta = 2.37$ (t, 1H), 4.04 (d, 2H), 4.31 (s, 2H), 4.08 (t, 5H, Cp), 4.17 (t, 2H, Cp), 4.23 (t, 2H, Cp); ¹³C NMR (CDCl₃, 22 °C): $\delta = 79.96$ (C \equiv C), 82.34 (C \equiv C), 56.46 (OCH₂), 67.61 (OCH₂), 69.54 (Cp), 68.64 (Cp), 68.01 (Cp); IR (hexane): 2171 ν (C \equiv C), 3296 ν (C=C–H) cm⁻¹. Anal. Calc. for C₁₄H₁₄FeO: C, 66.17; H, 5.55. Found: C, 64.85; H, 5.87%.

4.3. Synthesis of Fc(CH₂OCH₂C \equiv CH)₂, **3**

A solution of **1b** (1 g, 4.06 mmol) in 15 ml DMSO was treated with NaOH (0.406 g, 10.15 mmol) at room temperature for 30 min. Propargyl bromide (1.34 ml, 12.18 mmol) was added dropwise to the reaction mixture and stirred for 24 h. Reaction mixture was diluted with 10–15 ml of cold water and extracted with EtOAc. The organic layer was dried over anhydrous Na₂SO₄ and removed under reduced pressure. The pure product was isolated by silica gel column chromatography and elution with EtOAc:hexane (30:70 v/v) yielded yellow Fc(CH₂OCH₂C \equiv CH)₂, **3** (0.74 g, 56%).

4.3.1. Compound **3**

MS (FAB) P⁺(max): *m/z* (%) 323; ¹H NMR (400 MHz, CDCl₃, 22 °C): $\delta = 2.46$ (t, 2H), 4.13 (d, 4H), 4.37 (s, 4H), 4.16 (t, 4H, Cp), 4.23 (t, 4H, Cp); ¹³C NMR (CDCl₃, 22 °C): $\delta = 78.85$ (C \equiv C), 81.9 (C \equiv C), 55.59 (OCH₂), 66.39 (OCH₂), 68.3 (Cp), 68.83 (Cp); IR (hexane): 2121 ν (C \equiv C), 3225 ν (C=C–H) cm⁻¹. Anal. Calc. for C₁₈H₁₈FeO₂: C, 67.10; H, 5.63. Found: C, 68.01; H, 6.14%.

5. X-ray structure determination

Suitable X-ray quality crystals of **2** and **3** were grown by slow diffusion of a hexane:CH₂Cl₂ (6:4 v/v) solution and single crystal X-ray diffraction studies were undertaken. X-ray single crystal data were collected using Mo K α ($\lambda = 0.71073 \text{ \AA}$) radiation on a BRUKER APEX II diffractometer equipped with CCD area detector. Data col-

lection, data reduction, structure solution/refinement were carried out using the software package of SMART APEX. All structures were solved by direct method and refined in a routine manner. In most of the cases, nonhydrogen atoms were treated anisotropically. Whenever possible, the hydrogen atoms were located on a difference Fourier map and refined. In other cases, the hydrogen atoms were geometrically fixed.

5.1. Crystal data for **2**

Formula, C₁₄H₁₄FeO; Crystal system, space group: Monoclinic, P2₁/c. Unit cell dimensions, $a = 13.9336(13) \text{ \AA}$, $b = 7.6206(7) \text{ \AA}$, $c = 10.6460(9) \text{ \AA}$, $\beta = 97.529(3)^\circ$; $Z = 4$. Density (calculated) 1.506 Mg/m³. Final *R* indices [$I > 2\sigma(I)$] $R_1 = 0.0449$, $wR_2 = 0.1145$. Index ranges $-18 \leq h \leq 17$, $-10 \leq k \leq 9$, $-11 \leq l \leq 14$. Crystal size $0.20 \times 0.12 \times 0.06 \text{ mm}^3$. Reflections collected 12182, independent reflections 2616, [R_{int}] = 0.0529, Goodness-of-fit on F^2 1.073.

5.2. Crystal data for **3**

Formula, C₁₈H₁₈FeO₂; Crystal system, space group: Monoclinic, P2₁/n. Unit cell dimensions, $a = 10.1852(3) \text{ \AA}$, $b = 7.7449(2) \text{ \AA}$, $c = 10.4820(3) \text{ \AA}$, $\beta = 117.3080(10)^\circ$; $Z = 2$. Density (calculated) 1.456 Mg/m³. Final *R* indices [$I > 2\sigma(I)$] $R_1 = 0.0258$, $wR_2 = 0.0696$. Index ranges $-13 \leq h \leq 13$, $-10 \leq k \leq 10$, $-13 \leq l \leq 12$. Crystal size $0.42 \times 0.38 \times 0.15 \text{ mm}^3$. Reflections collected 5484, independent reflections 1826, [R_{int}] = 0.0187, Goodness-of-fit on F^2 1.063.

6. Supplementary material

CCDC 747629 and 747630 contain the supplementary crystallographic data for **2** and **3**. These data can be obtained free of charge from The Cambridge Crystallographic Data Centre via www.ccdc.cam.ac.uk/data_request/cif.

Acknowledgements

The authors thank Prof. Amitabha Sarkar and Prof. Parthasarathi Dastidar of the Indian Association for the Cultivation of Science for their encouragement and helpful discussions. The authors also thank Prof. M.V. Sangaranarayanan and A. Muthukrishnan for helpful discussions on electrochemical study. Generous support of the Council of Scientific and Industrial Research (CSIR), New Delhi, is gratefully acknowledged. We also thank Mass lab, SAIF, CDRI, Lucknow 226001, INDIA for FAB mass analysis. A.T. thanks the Council of Scientific and Industrial Research (CSIR), India, for a Junior Research Fellowship.

References

- [1] G.A. Jeffrey, An Introduction to Hydrogen Bonding, Oxford University Press, New York, 1997.
- [2] S. Scheiner, Hydrogen Bonding, Oxford University Press, New York, 1997.
- [3] G.R. Desiraju, T. Steiner, The Weak Hydrogen Bond in Structural Chemistry and Biology, Oxford University Press, Oxford, UK, 1999.
- [4] T. Steiner, Angew. Chem., Int. Ed. 41 (2002) 48.
- [5] H.-C. Weiss, D. Blaser, R. Boese, B.M. Doughan, M.M. Haley, Chem. Commun. (1997) 1703.
- [6] J.M.A. Robinson, B.M. Kariuki, K.D.M. Harris, D. Philp, J. Chem. Soc., Perkin Trans. 2 (1998) 2459.
- [7] A.J. Deeming, G. Hogarth, M.-Y. Lee, M. Saha, S.P. Redmond, H. Phetmumg, A.G. Orpen, Inorg. Chim. Acta 309 (2000) 109.
- [8] A. Dey, R.K.R. Jetti, R. Boese, G.R. Desiraju, Cryst. Eng. Commun. 5 (2003) 248.
- [9] P.J. Langley, J. Hulliger, R. Thaimattam, G.R. Desiraju, New J. Chem. 22 (1998) 1307.
- [10] F. Barriere, W.E. Geiger, J. Am. Chem. Soc. 128 (2006) 3980.
- [11] M.I. Bruce, P.J. Low, F. Hartl, P.A. Humphrey, P. Montigny, M. Jevric, C. Lapinte, G.J. Perkins, R.L. Roberts, B.W. Skelton, A.H. White, Organometallics 24 (2005) 524.
- [12] R.C.J. Atkinson, V.C. Gibson, N.J. Long, Chem. Soc. Rev. 33 (2004) 213.

- [13] D.R. van Staveren, N.-M. Nolte, *Chem. Rev.* 104 (2004) 5931.
- [14] R.G. Arrayas, J. Adrido, J.C. Carretero, *Angew. Chem., Int. Ed.* 45 (2006) 7674.
- [15] P. Zanello, in: A. Togni, T. Hayshi (Eds.), *Ferrocenes: Homogenous Catalysis Organic Synthesis Materials Science*, VCH, Weinheim, 1995.
- [16] O.B. Sutcliffe, M.R. Bryce, *Tetrahedron: Asymmetry* 14 (2003) 2297.
- [17] N.J. Long, *Metallocenes*, 1st ed., Blackwell Science, London, 1997.
- [18] J.F.M. da Silva, M. Zaslhoff, *Nature* 415 (2002) 389.
- [19] M.A. Schmitt, B. Weisblum, S.H. Gellman, *J. Am. Chem. Soc.* 126 (2004) 6848.
- [20] S. Fernandes-Lopes, H.S. Kim, E.C. Choi, M. Delgado, J.R. Granja, A. Khasanov, K. Kraehenbuehl, G. Long, D.A. Weinberger, K.M. Wilcoxon, M.R. Ghadiri, *Nature* 412 (2001) 452.
- [21] H. Yan, A.M. Beatty, T.P. Fehlner, *J. Organomet. Chem.* 691 (2006) 5060.
- [22] W.-Y. Wong, W.-K. Wong, P.R. Raithby, *J. Chem. Soc., Dalton Trans.* (1998) 2761.
- [23] W.-Y. Wong, G.-L. Lu, K.-F. Ng, K.-H. Choi, Z. Lin, *J. Chem. Soc., Dalton Trans.* (2001) 3250.
- [24] R.D. Adams, B. Qu, M.D. Smith, *Organometallics* 21 (2002) 4847.
- [25] W.-Y. Wong, K.-Y. Ho, K.-H. Choi, *J. Organomet. Chem.* 670 (2003) 17.
- [26] R.D. Adams, O.-S. Kwon, B. Qu, M.D. Smith, *Organometallics* 20 (2001) 5225.
- [27] W.-Y. Wong, K.-Y. Ho, S.-L. Ho, Z. Lin, *J. Organomet. Chem.* 683 (2003) 341.
- [28] B. Bildstein, M. Schweiger, H. Kopacka, K. Wurst, *J. Organomet. Chem.* 553 (1998) 73.
- [29] W. Skibar, H. Kopacka, K. Wurst, C. Salzmann, K.-H. Ongania, F.F. de Biani, P. Zanello, B. Bildstein, *Organometallics* 23 (2004) 1024.
- [30] K.N. Jayaprakash, R.C. Pares, I. Matsuoka, M.M. Bhadbhade, V.G. Puranik, P.K. Das, H. Nishihara, A. Sarkar, *Organometallics* 18 (1999) 3851.
- [31] M. Nishio, *Cryst. Eng. Commun.* 6 (2004) 130.
- [32] M. Nishio, Y. Umezawa, K. Honda, S. Tsuboyamad, H. Suezawa, *Cryst. Eng. Commun.* 11 (2009) 1757.
- [33] D.W. Hall, C.D. Russel, *J. Am. Chem. Soc.* 89 (1967) 2316.
- [34] W.F. Little, J.D. Johnson, A.P. Sanders, C.N. Reilley, *J. Am. Chem. Soc.* 86 (1964) 1382.
- [35] G.G.A. Balavoine, G. Doisneau, T. Fillebeen-Kha, *J. Organomet. Chem.* 412 (1991) 381.
- [36] U.T.M. Westerhoff, Z. Yang, G. Ingram, *J. Organomet. Chem.* 463 (1993) 163.